

# Diffuse Ionized Gas inside the dwarf irregular galaxy NGC 6822<sup>1</sup>

A.M. Hidalgo-Gómez

*Instituto de Astronomía, Universidad Nacional Autónoma de México, Ciudad  
Universitaria, Aptdo. 70 264, C.P. 04510, Mexico City, Mexico*

*and*

*Escuela Superior de Física y Matemáticas, IPN, U.P. Adolfo López Mateos, Mexico City,  
Mexico*

and A. Peimbert

*Instituto de Astronomía, Universidad Nacional Autónoma de México, Ciudad  
Universitaria, Aptdo. 70 264, C.P. 04510, Mexico City, Mexico*

## ABSTRACT

We have studied the differences between the diffuse ionized gas (DIG) and the H II regions along a slit position in the local dwarf irregular galaxy NGC 6822. The slit position passes through the two most prominent H II regions: Hubble V and Hubble X. Important differences have been found in the excitation, ionization, and  $[\text{N II}]\lambda 6584\text{\AA}/\text{H}\alpha$  and  $[\text{S II}]\lambda 6717\text{\AA}/\text{H}\alpha$  line ratios between the DIG and the H II locations. Moreover, the values of all the line ratios are not similar to those in the DIG locations of spiral galaxies but are very similar to the values in other irregular galaxies, such as IC 10. We also determined the rate of recombination using the He I  $\lambda 5875$  line. Finally, we obtained a picture of the ionization sources of the DIG. We consider that the leakage of photons from the H II regions might explain most of the line ratios, except  $[\text{N II}]/\text{H}\alpha$ , which might be explained by turbulence.

## 1. Introduction

The study of the diffuse ionized gas (DIG) in irregular galaxies is very difficult, mainly due to the difficulties in distinguishing between proper H II regions and other regions of ionized gas with very low density. In spiral galaxies the diffuse gas is very easy to detect,

---

<sup>1</sup>Based on observations collected at the European Southern Observatory, Chile, proposal number 69.C-0203(A)

as it is located either above the disc or in the interarm regions, neither of which exists in irregular galaxies. Consequently, such studies have been carried out for very few irregular galaxies. Hunter & Gallagher (1994) solved this problem by studying the emission at the edges of a few irregular galaxies, while Martin (1997) in her sample did not put hard limits on the line ratios of either group. So far, all the places with ionized gas have been identified as H II regions, especially when only H $\alpha$  images were used (e.g. Hodge et al. 1989). Therefore, DIG locations in an H $\alpha$  image might be mistaken for low-excitation H II regions.

In a previous study of the DIG in irregular galaxies (Hidalgo-Gómez 2005, 2006), a distinction was made between DIG and H II regions. Such a distinction is important due to the different spectral characteristics of the H II and DIG locations: DIG exhibits lower excitation and larger [N II] $\lambda$ 6584Å/H $\alpha$  and [S II] $\lambda$ 6717Å/H $\alpha$  ratios. Such differences were first observed in spiral galaxies (e.g. Rand 1998; Tüllman & Dettmar 2000) and then confirmed in irregular galaxies (Hidalgo-Gómez 2005, 2006). Hidalgo-Gómez & Ramírez-Fuentes (2006) have shown how the inclusion of DIG locations as part of an H II region has a drastic influence on the metallicity of the region. Moreover, when a proper comparison is made between the DIG in spiral and in irregular galaxies, it becomes clear that they are very different. This difference could be due to differences in the metallicity and the electronic temperature, as well as in the dust content and gas mass in both types of galaxies. However, the mechanisms involved in the ionization of this low-density gas might also be different. So it is very important to disentangle real H II regions from DIG in order to obtain reliable conclusions.

At this stage of the investigation of the DIG properties in irregular galaxies, we are interested in comparing the line ratios found in irregular galaxies to those in spirals. Also, we verify whether the present models, obtained specifically for the Milky Way and other high-metallicity spirals, can also explain the spectral lines in irregular galaxies. If there are any differences that are related to global properties of the interstellar medium (ISM), such as the metal abundance or the star formation rate (SFR), they could be of the utmost importance in the evolution of galaxies. Such relationships are studied elsewhere (Hidalgo-Gómez 2006).

In the present investigation we study the DIG inside NGC 6822. This is a close galaxy ( $d \approx 500$  kpc; Karachentsev 2005), defined by de Vaucouleurs et al. (1991) as a barred irregular with an oxygen abundance slightly lower than that of the Large Magellanic Cloud (LMC; Hidalgo-Gómez et al. 2001, hereafter HGOM01; Peimbert et al. 2005). It is a small galaxy, with  $r_{25} = 1.08$  kpc (Hidalgo-Gómez & Olofsson 1998) but an extension on the sky of  $13.5' \times 15.5'$ . Hodge et al. (1989) found a total of 145 H II regions, some of which are extremely faint. The two brightest H II regions, -Hubble V and Hubble X, located in the northern part of the galaxy-, and the DIG in their vicinities are the targets here. The main reason is that they are very close to each other, separated only by 300 pc; both have very

similar metal content and ionizing stellar temperature (e.g. HGOM01). Therefore, the OB stellar populations should be very similar in both of them, as should the ionizing mechanisms of the regions. In addition, and contrary to what happens in IC 10, the SFR is low, of order of  $0.04 M_{\odot} \text{ yr}^{-1}$  (Wyder 2001), slightly lower than the typical values in irregular galaxies (Hunter & Elmegreen 2004); the existence of giant bubbles has not been reported there, although de Blok & Walter (2000) expressed that the H I is very disturbed. This galaxy, a very typical irregular galaxy, is in a sense an ideal candidate for comparing the ionization mechanics of the DIG among irregular galaxies and between irregulars and spirals.

The paper is structured as follows.: The information on the acquisition of the data, the reduction procedure, and the analysis of the data are given in Section 2. Section 3 describes the main characteristics of the DIG in the region. The ionization source is studied in Section 4, while a discussion on the possible geometry is given in Section 5. Finally, conclusions are outlined in Section 6.

## 2. Observations and data reduction

The data were long-slit observations acquired with the Focal Reducer/Low Dispersion Spectrograph, (FORS1), at the Melipal Very Large Telescope (VLT) in Cerro Paranal (Chile). The detector is a  $2048 \times 2048$  pixel CCD; it was used with an image scale of  $0.2''/\text{pixel}$  providing a slit length of  $5.8'$ . The slit width was set to  $0.51''$  and the slit orientation was almost east-west (position angle  $91^{\circ}$ ) in order to observe Hubble V and Hubble X simultaneously. Figure 1 shows the region under study, with the slit superimposed. Two grism settings were used in these observations: GRIS600B+12, which provided a spectral coverage in the  $3450\text{--}5900 \text{ \AA}$  range, and GRIS600R+14 with the filter GG435, which provided a spectral coverage in the  $5250\text{--}7450 \text{ \AA}$  range. The resolution for the emission lines observed with the blue grism is given by  $\Delta\lambda \sim \lambda/1300$ , while the resolution with the red grism is given by  $\Delta\lambda \sim \lambda/1700$ . There were three integrations, 12 minutes each, in the blue setting, and three integrations, 10 minutes each, in the red setting. The spectra were reduced following the standard procedure using the IRAF reduction package. Bias and sky twilight flat-fields were used for the calibration of the CCD response. Ne-Ar-He lamps were used for the wavelength calibration. The spectra were corrected for atmospheric extinction using the La Silla extinction law. Four standard stars were observed in order to perform the flux calibration. More details on the reduction procedure can be found in Peimbert et al. (2005).

These two spectra were divided into a total of 40 one-dimensional spectra, each being the average of 50 rows corresponding to  $10''$  on the sky. Although the seeing conditions were good enough, the low signal-to-noise (S/N) at very low surface brightness due to the small

width of the slit, produced a very large number of pixels. For each of these spectra, the intensity of the recombination lines  $H\alpha$  and  $H\beta$ , as well as the forbidden lines  $[O II] \lambda 3727$ ,  $[O III] \lambda 5007$ ,  $[N II] \lambda 6583$ ,  $[S II] \lambda 6717$ , and  $[S II] \lambda 6731$ , were measured. In addition, we obtained a total of five spectra (hereafter, referred as the integrated spectra), covering the two main  $H II$  regions and the three DIG regions: two at the edge of the slit (DIG E and DIG W) and the third one in between the two  $H II$  regions (DIG C). The lengths of these integrated spectra were as follows: DIG E=30", Hubble X=40", DIG C=130" Hubble V=50" and DIG W=150". For these five spectra, the helium recombination line at 5876Å was also measured, in addition to the previously mentioned lines.

The lines in both sets of spectra were normalized to  $H\beta$ , absorption-corrected following McCall et al. (1985) and extinction-corrected using

$$C_\beta = -\frac{1}{f(\lambda) - f(H\beta)} \ln \left[ \frac{I(\lambda_o)/I(H\beta_o)}{I(\lambda)/I(H\beta)} \right]$$

where  $I(\lambda_o)/I(H\beta_o)$  is the observed intensity of the line relative to  $H\beta$ ,  $I(\lambda)/I(H\beta)$  is the theoretical value determined for an optically thick gas (Brocklehurst 1971), and  $f(\lambda)$  is the adopted extinction law; in this paper we used the Whitford modified law (Savage & Mathis 1979). One caveat in the extinction correction is the  $H\beta$  absorption in the stellar continuum present at most DIG locations. This underlying absorption can significantly change the  $H\beta$  emission intensity. Therefore, the extinction might be somewhat artificial, and  $C_\beta$  can produce odd values of the line intensities, especially  $[O II] \lambda 3727$ . As can be seen, the values of these coefficients inside the  $H II$  regions do not match the previous ones (HGOM01; Peimbert et al. 2005). In this investigation the extinction-corrected intensities are preferred. Those ratios for which the differences between the reddened and non-reddened intensities are important (up to 30%), such as  $[O II]/H\beta$ ,  $[O II]/H\alpha$ , and  $[O III]/H\alpha$ , are not considered.

After these corrections, the line ratios  $[O III] \lambda 5007/H\beta$ ,  $[N II] \lambda 6584/H\alpha$ ,  $[S II] \lambda 6717/H\alpha$ ,  $[N II] \lambda 6584/[S II] \lambda 6717$ , and  $[S II] \lambda 6717/[S II] \lambda 6731$  were determined for both, the one-dimensional and the integrated spectra sets. In the latter, the  $He I \lambda 5876/H\alpha$  ratio was also determined. As this helium line blends with a sky line, the values tabulated here might be slightly larger than the real ones. These values are given in Table 1 for the integrated spectra, with their uncertainties. The formal errors were determined from

$$\sigma_t = (\sigma_c^2 + \sigma_r^2 + \sigma_a^2)^{1/2}$$

with  $\sigma_c$  representing the uncertainties at the level of the spectral continuum with respect to the line;  $\sigma_r$  are those uncertainties introduced by the reduction procedure, and  $\sigma_a$  are the uncertainties due to the extinction and absorption corrections. They are of order less than

5%. Another 10% was added to the uncertainties of the line ratios based on the differences between the low-density limit,  $[\text{S II}] \lambda 6717/[\text{S II}] \lambda 6731 = 1.44$  (Osterbrock 1989), and the density at the DIG locations. The variations in the continuum in the vicinity of the helium line increase the uncertainties up to 50%, but the line is clearly detected.

### 3. Diffuse Ionized Gas inside NGC 6822

The best parameter for defining the DIG is the density. But density is also one of the most difficult parameters to determine from long-slit spectroscopy data, especially in the low-density regime. The main problem is that in this regime, the differences in the  $[\text{S II}] \lambda 6717/[\text{S II}] \lambda 6731$  ratio between the H II regions, with typical densities of  $100 \text{ cm}^{-3}$ , and the DIG with values of  $10 \text{ cm}^{-3}$ , are of order 0.1 (see Fig. 5.3 in Osterbrock 1989), which normally is smaller than the uncertainties in the ratio. Therefore, another parameter has to be used for the definition of DIG.

The most important parameter after the density is the emission measure ( $EM$ ) (Greenawalt et al. 1998) related to the surface brightness in  $\text{H}\alpha$  by the expression

$$EM = (7.22 \times 10^{13}) SB(H\alpha) T^{0.96}$$

, where  $T$  is the electronic temperature and  $SB(H\alpha)$  is the surface brightness in  $\text{H}\alpha$  in  $\text{ergs cm}^{-2} \text{ s}^{-1} \text{ arcsec}^{-2}$  (M. Richer 2001, private communication). This equation is equivalent to other formulations existing in the literature (Reynolds et al. 1999). In spiral galaxies, values of  $EM$  between  $2$  and  $100 \text{ cm}^{-6} \text{ pc}$  have been considered (Greenawalt et al. 1998; Reynolds 1984). In previous studies of the DIG, values of  $EM = 2 \text{ cm}^{-6} \text{ pc}$  for IC 10 DIG locations (Hidalgo-Gómez 2005) and  $EM = 8 \text{ cm}^{-6} \text{ pc}$  for GR 8 and ESO 245-G05 DIG locations (Hidalgo-Gómez 2006) were determined using the cumulative function of the surface brightness in  $\text{H}\alpha$ , with Galactic extinction corrected. A similar approach has been taken here. On Figure 2 this function with the data of NGC 6822 is shown. Two straight lines can be fitted to this curve. The intersecting point corresponds to the surface brightness [hereafter referred to as  $SB(H\alpha)$ ], which divides the sample into H II regions and DIG. In Figure 2 this point is located at  $5 \times 10^{-16} \text{ ergs cm}^{-2} \text{ s}^{-1} \text{ arcsec}^{-2}$ . This surface brightness gives an  $EM \approx 200 \text{ cm}^{-6} \text{ pc}$  for  $10,000 \text{ K}$  (see Table 1). This value is much larger than the values obtained for the galaxies studied so far for similar values of  $T_e$ , and only similar to the value in DDO 50 (A.M. Hidalgo-Gómez 2007, in preparation).

Using this surface brightness, we have divided the 40 spectra into two groups: 31 are DIG locations and 9 are H II regions. It has to be realized that because of the large size of the spectra (50 rows), H II regions may include a part of the DIG and vice versa. The

H II regions of  $\approx 150$  and  $125$  pc (projected sizes), correspond to Hubble V and Hubble X, respectively. These sizes are comparable to the sizes of the regions obtained in previous studies (HGOM01).

In Table 1, the line ratios measured from the integrated spectra are listed for the three DIG and the H II locations. Along with them, the extinction parameter as described previously, the S/N in the  $H\alpha$  line, and the electronic temperature of the DIG are shown. The electronic temperature in the DIG was obtained using both oxygen and nitrogen lines. For the oxygen temperature we assumed an abundance of 8.34 (Peimbert et al. 2005) and  $T([O II]) = T([O III])$  and searched for the temperature that would reproduce the intensities of  $[O II]\lambda 3727$ . For the nitrogen temperature we assumed an abundance of 7.05 (Peimbert et al. 2005) and a nitrogen degree of ionization equal to that of oxygen.

### 3.1. DIG along the slit position

Figures 3-6 present values along the slit of the  $SB(H\alpha)$ , the excitation, the ionization,  $[N II] \lambda 6584/H\alpha$ , and  $[S II] \lambda 6717/H\alpha$ . All the plots follow a similar structure: in the  $x$ -axis the spatial extension of the region under study is plotted from the east to the west of the galaxy. The line ratios under consideration are shown at the  $y$ -axis. The dotted lines contain the H II regions. In all except Figure 3 the values of the integrated spectra are shown (*dashedline*), and the dot-dashed lines correspond to their uncertainties.

Figure 3 gives the log of the surface brightness in the  $H\alpha$  line. The most interesting feature is the relatively constant SB for the DIG locations. The H II regions are clearly defined by their higher SB.

Figure 4 shows the excitation, defined as  $[O III]\lambda 5007/H\beta$ , along the slit. Hubble V, located between  $200''$  and  $250''$ , has a larger excitation than Hubble X (between  $30''$  and  $70''$ ), which is in agreement with previous investigations (HGOM01). For both the DIG and H II regions the excitation from the integrated spectra agrees with the values from the one-dimensional spectra when error bars are taken into account. The typical error bar of the latter spectra in both H II regions is 11%. For the DIG locations error bars are larger: as high as 21%. The error bars are not shown in the figures for the sake of clarity. Considering the DIG locations, their excitation is higher than the results obtained from spiral galaxies (e.g. M31; Greenawalt et al. 1998). Actually, only eight locations have values of  $[O III]/H\beta$  smaller than 1, and only in one location is it smaller than 0.6, at  $275''$ . Although this excitation is very high, other irregular galaxies have similar (DDO 53; Hidalgo-Gómez & Flores-Fajardo 2007) or even larger (IC 10; Hidalgo-Gómez 2005) values.

Concerning the DIG integrated spectra, the larger values of the excitation correspond to the region named DIG E. This region was averaged over only 125 rows and therefore has a S/N lower than the other two DIG regions. Therefore, and considering the similar value of the excitation between regions W and C, the excitation might be overestimated in region E.

Another important feature is the large peak between  $130''$  and  $150''$ . It cannot be due to an excitation increment at these locations because the intensity of the [O III]  $\lambda 5007$  line is approximately constant. On the contrary, the intensity of  $H\beta$  drops by a factor of 4 and 3, respectively, in these two spectra. The best explanation could be a severe absorption in the  $H\beta$  intensity. Actually, a nebular condensation is clearly seen in Figure 1 in this place (marked as "1"), which might be a young stellar cluster. A value of 1.20 is obtained for the integrated spectra of DIG C when this region is excluded. This is consistent within the error bars with the value listed in Table 1. By comparing Figures 3 and 4, it is clearly seen that those locations with high  $SB(H\alpha)$  are also those with the larger excitation, which actually correspond to the H II regions.

The ratios [N II]  $\lambda 6584/H\alpha$  and [S II]  $\lambda 6717/H\alpha$  are very interesting because DIG in spiral galaxies has very high values for them (Otte & Dettmar 1999). Those ratios are shown in Figures 5 and 6, respectively. In both cases, there is a large increment of these ratios at the DIG locations. The values of the H II regions are very small, but in perfect agreement with more detailed investigations of these two regions (HGOM01). Some of the one-dimensional spectra show large differences compared to the integrated spectra in [NII]/ $H\alpha$ . Examples include the spectrum at  $330''$ - $340''$  with [NII]/ $H\alpha$  of  $0.2 \pm 0.1$ , and the spectrum at  $160''$  with [NII]/ $H\alpha$  of  $0.09 \pm 0.01$ . The reason for such discrepancy is likely the low S/N of the one-dimensional spectra (Rola & Pelat 1994). The [NII]/ $H\alpha$  ratio from the integrated spectra is almost identical for DIG C and W and the majority of the one-dimensional spectra of DIG C and W agree well with the integrated spectra values, when error bars are considered. Such error bars could be as high as 30% in some of the one-dimensional spectra.

[S II]  $\lambda 6717/H\alpha$  is a ratio related to shocks (Dopita 1993). For very large values ( $> 0.3$ ), shocks must be important contributors to the intensity of this ratio. Two things can be noted from Figure 6: first, the values are very small, the higher value being  $0.15 \pm 0.09$ ; there are no spectra along the slit where this ratio is large enough for shocks to be important. Second, although the ratio is larger in DIG locations than inside the H II regions by a factor of 3, in the former the ratio is very constant, considering the uncertainties. Without the reddening correction, the ratio is slightly larger (by 0.02), especially at low  $SB(H\alpha)$  locations. As for the [N II]/ $H\alpha$  ratio, there are some discordant one-dimensional spectra in the [S II]/ $H\alpha$  ratio at  $135''$ ,  $275''$ , and  $355''$ , with values of  $0.095 \pm 0.03$ ,  $0.15 \pm 0.04$ , and  $0.09 \pm 0.03$ , respectively. When uncertainties in these spectra are considered ( $\approx 30\%$ ), they agree with the integrated

spectra values. Again, the  $[\text{S II}]/\text{H}\alpha$  ratios in DIG C and W are almost identical.

The ratio  $[\text{S II}] \lambda 6717/[\text{S II}] \lambda 6731$  related to the density (Osterbrock 1989) has also been studied. But because one-third of the data go beyond the low-density limit, this plot is not shown. The same occurs for the integrated spectra (see Table 1). Another important feature is the uniformity of this ratio along the slit, showing no differences between DIG and H II locations. Therefore, it can be concluded that every place along the slit has very low density ( $n_e < 200 \text{ cm}^{-3}$ ). Actually, very low density values are found inside the H II regions from the  $[\text{O II}]$  and  $[\text{Cl III}]$  doublets (Peimbert et al. 2005).

## 4. On the search for the ionization source

### 4.1. Photoionization

According to Strömgren (1939), H II regions could be radiation- or density-bounded. If all the energy of the ionizing photons is used to ionize the atoms, the H II region is referred to as radiation-bounded. On the contrary, when the photons at the edge of the region still have enough energy to ionize atoms, it is called a density-bounded region.

Considering H II regions as radiation-bounded, Mathis (1986) and Domgörgen & Mathis (1994) made some predictions on the DIG line ratios: large values for both  $[\text{S II}] \lambda 6717+6731/\text{H}\alpha$  and  $[\text{N II}] \lambda 6584/\text{H}\alpha$  ( $> 0.3$ ), very large  $[\text{O II}]/\text{H}\alpha$  ( $> 1$ ) values, and very small  $[\text{O III}]/\text{H}\alpha$  ( $< 0.1$ ) and  $\text{He I}/\text{H}\alpha$  ( $< 0.03$ ) values. We can compare them with the values from Table 1. The  $[\text{O II}]/\text{H}\alpha$  and  $[\text{O III}]/\text{H}\alpha$  ratios are not used due to the extinction problems previously discussed. None of the other three lines has the value predicted by these photoionization models. The main weakness is that the models were optimized for Milky Way metallicity, whereas NGC 6822 has a metallicity  $\approx 1/30 Z_\odot$ . Castellanos et al. (2004) and Elwert & Dettmar (2005) used the photoionization code CLOUDY with different input parameters and lower metallicities in order to reproduce the line ratios observed. Both are successful in reproducing the rise of the  $[\text{N II}]$  versus  $[\text{S II}]$  plot, but none of them can fit the excitation. When Monte Carlo simulations with different ionizing spectra and metallicities are performed (Wood & Mathis 2004), a similar situation takes place.

Another prediction of the photoionization models is the relatively constant  $[\text{N II}] \lambda 6584/\text{H}\alpha$  line ratio between the DIG and H II regions. From Figure 5 it can be seen that it does not happen here; in fact, there are strong variations along the slit. Such variations can be due to differences in the content of nitrogen or in the electronic temperature. Thus, for example, differences of 600 K in the  $T_e$  can explain the small value of the spectrum at  $165''$ . Such differences, although large, are in fact observed in the outer part of Hubble V and Hubble X



(see Fig. 8 in HGOM01). Therefore, they cannot be ruled out as a source of inhomogeneity in the  $[\text{N II}] \lambda 6584/\text{H}\alpha$  ratio.

Although classical photoionization models cannot explain the line ratios observed in NGC 6822, the correlation between  $[\text{N II}]$  versus  $[\text{S II}]$  and the recombination rates does not allow us to rule out these models completely. The strong correlation observed in the DIG of spiral galaxies between  $[\text{N II}] \lambda 6583$  and  $[\text{S II}] \lambda 6717$  indicates that the  $[\text{N II}]/[\text{S II}]$  ratio is constant (e.g. Otte & Dettmar 1999; Rand 1998). Such a constancy cannot be explained by classical photoionization models (Hoopes & Walterbos 2003). Using this result, Otte et al. (2001, 2002) derived an increase of temperature toward the halo that can be reproduced with the multidimensional photoionization simulations of the density-bounded H II regions of Wood & Mathis (2004). They concluded that the increase with distance from the plane observed in spiral galaxies is due to hardening of the radiation field with  $z$ . Such a correlation is not observed for any of the dwarf irregular galaxies studied so far (Hidalgo-Gómez 2005; 2006; Hidalgo-Gómez & Flores-Fajardo 2007; A.M. Hidalgo-Gómez 2007, in preparation). In Figure 7 this relationship is shown for this galaxy. A strong correlation is obtained for the H II regions (*diamonds*), with a regression coefficient of 0.99 but only nine data points, while DIG locations (*asterisk*) show a vertical line. The explanations could be several: one might be related to the fact that the locations with larger  $[\text{N II}] \lambda 6584/\text{H}\alpha$  also might have larger excitation. Therefore, and since the ionization parameter of  $\text{S}^{++}$  is smaller than that of  $\text{O}^{++}$ , most of the  $\text{S}^+$  has been ionized into  $\text{S}^{++}$ , which is the reason for the behaviour of the DIG data points in Figure 7 (M. Peimbert 2005, private communication). Figure 8 shows the relation between  $\log([\text{N II}] \lambda 6584/\text{H}\alpha)$  and  $\log([\text{O III}] \lambda 5007/\text{H}\beta)$ . A strong correlation for the DIG data point is expected if the above reasoning explains the lack of correlation. On the contrary, there is a stronger correlation for H II regions, while only a weak trend is observed for the DIG data points. Other explanations have to be invoked: a difference in the chemical content of any of these ions, or effects due to the different ionization level of these two species (Petuchowski & Bennet 1993, 1995), may account for the variations observed in Figure 7. However, if the correlation is due to  $T_e$ , as in Wood & Mathis (2004), Figure 7 indicates that the temperature of the DIG is quite homogeneous, while significant differences are found in the H II regions. Figure 8 in HGOM01 shows that such differences in the temperature are present inside these H II regions, especially inside Hubble V.

The second disconcerting factor is the high recombination rate determined from the He I  $\lambda 5876$  line, following the expression (e.g. Miller & Veilleux 2003)

$$\frac{\Xi_{\text{He}}}{\Xi_{\text{H}}} = \frac{0.052(\frac{N_p}{N_{\text{He}^+}})(\frac{T_e}{8000})^{0.14}}{0.048(\frac{\text{He}/\text{H}}{0.1})}$$

where  $\Xi_{\text{He}}$  and  $\Xi_{\text{H}}$  are the emissivities of helium and hydrogen, respectively,  $T_e$  is the elec-

tronic temperature,  $He/H$  is the helium abundance, and  $0.052N_p/N_{He^+}$  comes from the emissivities of the hydrogen and helium recombination lines (Osterbrock 1989). The He abundances have been determined as  $He^+/H\alpha$  because, as mentioned before,  $H\beta$  might suffer from severe absorption. The electronic temperature is from Table 1. Recombination rates at the DIG locations between 0.65 and 1 are found, depending on the density of protons relative to  $He^+$  and  $T_e$ , indicating that photoionization is important there.

In recent years, leaky models have been proposed to explain the line ratios observed at the DIG. Hoppes & Walterbos (2003) and Wood & Mathis (2004) used density-bounded H II regions in their models, as did Domgörgen & Mathis (1994). In this case, there is not enough nearby neutral gas to absorb the total Lyman continuum of the source and form a classical Strömgren sphere. Wood & Mathis (2004) focused on explaining the constant  $[N II]/[S II]$  ratio (not observed in NGC 6822). They also used the  $[O III]/H\alpha$  ratio, which is very much affected by extinction. Moreover, although the  $[O III]/H\alpha$  increases by a factor of 2 in their models of density-bounded regions at low metallicities, as shown in their Figure 12, the values of their models for the other line ratios are not low enough to fit our results listed in Table 1. Therefore, such model is not used hereafter. In addition, the values obtained from the Domgörgen & Mathis (1994) model do not fit any of the line ratios obtained for NGC 6822.

The values of the  $[O III]/H\beta$ ,  $[N II]/H\alpha$  and  $[S II]/H\alpha$  ratios of the DIG from Table 1 are compared with the leakage models from Hoopes & Walterbos (2003). We make use of their Figure 14, in which they calculate the line ratios only for Orion metallicity and  $\log q = -3$ , where  $q$  is related to the ionization parameter. The  $He I/H\alpha$  ratio is not used, as our values lies outside the reach of the models. Moreover, several facts have to be remembered: due to the smaller metallicity of NGC 6822, some corrections to these models have to be carried out. The effect of lower metallicities increases the value of  $q$ , which in turn implies larger excitation and ionization. Moreover, irregular galaxies normally show a deficiency in nitrogen as compared to spirals (Hidalgo-Gómez & Olofsson 2002). As a consequence, the models predict a higher  $[N II] \lambda 6584/H\alpha$  line ratio than that observed in NGC 6822. Finally, a leakage of photons produces a harder spectrum and, therefore, larger values of the  $[O III]/H\beta$  (and  $[O II]/H\beta$ ) at lower  $T_{ion}$ . In addition, and because of the smaller S/N of DIG E, the values of DIG W and C, if they differ, are preferred.

As the excitation is very similar for both DIG W and C, a value of 1.2 can be used. For such a value, a leakage from 45% at 38,000 K to 60% at 42,000 K is given by the model. The excitation of DIG E is much higher, with values of 41,000-50,000 K for the same leakage range. The ratio  $[S II] \lambda\lambda(6717+6731)/H\alpha$  is almost identical for DIG W and C: 0.12. For a  $T_{ion}$  of 40,000 K, the leakage is 30%, increasing up 45% for 30,000 K. Although DIG E has

a lower ratio, there is no difference in the numbers. Something similar happens for the  $[\text{N II}] \lambda 6584/\text{H}\alpha$  ratio, where differences in the ratio do not imply differences in  $T_{ion}$ . For the three regions, a leakage of only 30% at 30,000 K is obtained. Considering the arguments given above, a leakage of 40%-50% with temperatures of 35,000 K can fit both the excitation and the  $[\text{S II}]/\text{H}\alpha$ . Very similar values of 40%-50% of photon leakage were obtained by Relaño et al. (2002) for NGC 346, the most luminous H II region in the Small Magellanic Cloud. The main problem is that nitrogen cannot be fitted. Leakages of 40%-50% give  $[\text{N II}]/\text{H}\alpha$  ratios of 0.4-0.5, which are not observed at any location. An explanation could be the low nitrogen content in irregular galaxies.

Another important caveat is that the leakage might have no preferable direction, and therefore the region in between the two H II regions might receive a large number of photons. Therefore, larger values of the excitation,  $[\text{N II}] \lambda 6584/\text{H}\alpha$  and  $[\text{S II}] \lambda 6717/\text{H}\alpha$ , could be expected, which is not the case. On the contrary, there are no significant differences between the various DIG locations, either for the one-dimensional spectra or for the integrated ones. One might think that differences in the density will vary the leakage in different directions. As discussed above, we cannot say much about variations in the density. If it were larger in DIG C, then the leakage of photons would be less likely in that direction, leading to similar line ratios everywhere.

Finally, we should be concerned about some discrepancy between the values of the integrated spectra and the spectra along the slit. The main reason for the use of the former is the higher S/N ratio. It is well known that when the S/N is lower than  $\approx 5$ , the intensity of the line is overestimated (Rola & Pelat 1994). An S/N lower than 5 is typical for the one-dimensional spectra, and therefore we think that the line ratios of the integrated spectra are more reliable. In any case, we can do a double-check. First, we can obtain an average value from the one-dimensional spectra for each of the line ratios of interest. Both  $[\text{N II}]/\text{H}\alpha$  and  $[\text{S II}]/\text{H}\alpha$  are identical, and differences of 0.2 compared to the values listed in Table 1 are found in the  $[\text{O III}]/\text{H}\beta$ . There is no difference in the ionization temperature or the photon-leaking percentage from the Hoopes & Walterbos models.

The second approach is to obtain a range of values for  $T_{ion}$  and photon leaking for each of the one-dimensional spectra. Again, there are no differences compared to the results from the integrated spectra. Percentages between 40% and 60%, and values of  $T_{ion}$  between 38,000 and 41,000 K, are obtained for most of the DIG locations from the  $[\text{O III}]/\text{H}\beta$  ratio. Only three spectra (10%) have ionization temperatures larger than 41,000 K. Values of 30%-40% of photons leakage and of 30,000 to 36,000 K for  $T_{ion}$  are obtained from the  $[\text{S II}]/\text{H}\alpha$  ratio for all the one-dimensional spectra. Therefore, it can be concluded that the leakages and  $T_{ion}$  values found from the integrated spectra are correct for 90% of the DIG locations.

In any case, according to us a leaky model is the model that most successfully explains the line ratios observed in the DIG in NGC 6822. The values of the leakage obtained here are similar to those of other irregular galaxies (Hidalgo-Gómez 2005; 2006).

## 4.2. Other source of ionization

The only discordant point to the picture presented in 4.1 is the low value of the  $[\text{N II}]/\text{H}\alpha$  ratio. In order to fit it, an ionization source that radiates its energy at low ionization species is needed. The ideal model is the turbulence produced by the mixing of layers of different temperatures (Slavin et al. 1993). A model with depleted abundances, an intermediate temperature after mixing of 100,000K, and a cloud temperature of  $T_c = 10^4$  K will give values of  $[\text{S II}]/\text{H}\alpha$  of 0.15-0.17 and  $[\text{N II}] \lambda 6584/\text{H}\alpha$  of 0.09-0.11 for velocities of hot gas between 20 and 100  $\text{km s}^{-1}$ . These values are close to the values from the integrated spectra. The main problem is that the cold gas lines are broad with a non-Gaussian shape, something that was not observed.

Finally, it might be interesting to explore the existence of shock waves that might have some influence on the ionization. According to de Blok & Walter (2000), the H I appearance of NGC 6822 is very disturbed. There are two main features: a giant H I hole to the southeast and a cloud to the northwest, which might be interacting with the galaxy and possibly very important sources of shock waves. Even if both of them are far away from the region under study here, the disturbance of the ISM over the entire galaxy can amplify them.

The best line for studying shocks is  $[\text{O I}] \lambda 6300\text{\AA}$ . Unfortunately, this line was not detected in any of the DIG locations, and therefore the  $[\text{S II}]/\text{H}\alpha$  ratio must be used. This ratio has served for detecting shocks, e.g. bubbles around W-R stars (Polcaro et al. 1995). We can compare the values of this ratio with those from a shock model (Dopita & Sutherland 1995). According to them, the  $[\text{S II}] \lambda 6717/\text{H}\alpha$  ratio varies between 0.26 and 0.59 for shocks with velocities from 150 to 500  $\text{km s}^{-1}$ . When precursors are included in the model, those values become 0.18 and 0.33, respectively. As the observed ratio is lower than 0.15 (0.17 for non-reddening correction) at any location along the slit, it can be concluded that the disturbed ISM of this galaxy has very little impact on the ionization of the DIG at the position of our observations.

Another useful tool for determining the influence of shocks could be the diagnostic diagram  $\log [\text{S II}] \lambda\lambda(6717+6731)/\text{H}\alpha$  versus  $\log [\text{O III}]/\text{H}\beta$ . According to Veilleux & Osterbrock (1987), this is the best diagram to differentiate shocked and photoionized regions. In Figure 9 this diagram is shown for the data points considered in this investigation. In

addition, the track of Dopita & Sutherland’s (1995) model without precursors and corrected for the metallicity of NGC 6822 is also shown. It divides the plot into the shocked region (*totherightoftheline*) and the non-shocked one (*totheleftoftheline*). All the data points for both H II and DIG lie inside the non-shocked region. Therefore, it can be concluded that shocks are not the dominant ionization source of the DIG in NGC 6822.

## 5. Discussion

In this section we discuss the geometry of the DIG. The most likely disposition is a homogeneous disposition of the ionized gas in the region. Like in Orion (O’Dell 2001), it is also probable that the gas thickness in front of the H II region is much smaller than that at the back. The excitation and the density can be used to discriminate between these possibilities.

Unfortunately, there is much information that cannot be obtained from the  $[\text{S II}]\lambda 6717/[\text{S II}]\lambda 6731$  ratio due to the problems mentioned above (see Section 3). The excitation will show narrow peaks for the thin scenario. The thinner the layer, the narrower are the peaks. The main reason is that for a thin front layer, the contribution of the classical photoionization in the H II regions and their immediate vicinity is observed, while for a thick distribution it becomes diluted, making the photon-leakage ionization more important. Also, this scenario will produce smaller  $C_\beta$  values at the DIG locations. The main problem is that the  $C_\beta$  values can also contain a contribution from the underlying stellar absorption. It becomes more important as the EM gets smaller and also due to the intensity of  $\text{H}\beta$ . Consequently, a severe stellar absorption will cause a higher extinction at the DIG locations, just as a thick and homogenous distribution of the ionized gas will appear.

Figure 4 clearly shows that the peaks are narrow and do not extend very far from the H II regions. Therefore, no significant quantity of gas should be located in front of the regions, in order to dilute the excitation. In any case, in order to know the real geometry of the gas, more observations are needed, especially at radio and IR wavelengths. They will discriminate between the stellar absorption and a thick layer of gas in front of the regions.

## 6. Conclusions

In the present investigation we have studied the characteristics of the DIG in the northern part of the irregular galaxy NGC 6822 using long-slit spectroscopy from FORS1 at the VLT. In order to study the properties of this gas, first we have to distinguish between those

places that form part of the H II regions and those of the proper DIG. We used the cumulative function in the surface brightness in H $\alpha$ . This function shows a change in the slope that marks the transition between H II regions and DIG locations. The value obtained,  $\log \text{SB}(\text{H}\alpha) = -15.3$ , is larger than those obtained for other irregular galaxies studied, such as IC 10 (Hidalgo-Gómez 2005), but similar to the value for DDO 50 (A.M. Hidalgo-Gómez 2007, in preparation).

We have studied the excitation,  $[\text{N II}] \lambda 6584/\text{H}\alpha$ ,  $[\text{S II}] \lambda 6717/\text{H}\alpha$ , and  $[\text{S II}] \lambda 6717/[\text{S II}] \lambda 6731$  along the slit. NGC 6822 is a very typical irregular galaxy as far as the DIG properties are concerned. Neither  $[\text{N II}]/\text{H}\alpha$  nor  $[\text{S II}]/\text{H}\alpha$  has values higher than 0.3 at any location, while they are larger than 0.4 in half of the spiral galaxies (see Table 1 in Hidalgo-Gómez 2004). The excitation is very high. In fact, only three locations have  $[\text{O III}]/\text{H}\beta$  smaller than 1; in contrast, it is very small ( $\approx 0.1$ ) in those spirals where it has been measured (Galarza et al. 1999). Moreover, there is a weak correlation between  $[\text{N II}]/\text{H}\alpha$  and  $[\text{S II}]/\text{H}\alpha$  for the DIG locations.

Additionally, these ratios are useful for determining the ionization source(s) of the DIG. The line ratios are very different from the classical photoionization models (e.g. Domgörgen & Mathis 1994), but helium is completely ionized and the  $[\text{N II}]/\text{H}\alpha$  is too low. Therefore, the picture that might be more likely is the following: the helium is ionized in the vicinity of the H II regions while turbulence can increase the  $[\text{N II}]/\text{H}\alpha$  ratio. Both the  $[\text{O III}]/\text{H}\beta$  and  $[\text{S II}]/\text{H}\alpha$  are increased by photons escaping from the H II regions, which amounts to 40%-50%. Although the H I in NGC 6822 is very disturbed (de Blok & Walter 2000), the disturbances have no consequence for the ionization of the DIG at the locations of Hubble X and Hubble V.

Finally, it should be kept in mind that we are observing the result of all the processes simultaneously, and probably through a thick layer of neutral gas.

The authors are indebted to M. Peimbert and M. T. Ruiz for help with the observations and many fruitful discussions. A. M. H.-G. thanks M. Peimbert, who suggested including these data on the study of the DIG, and to many colleagues at Instituto de Astronomía-Universidad Nacional Autónoma de México for fruitful comments on this work. This investigation was partly supported by CONACyT project 2002-c40366 and DGAPA-UNAM grant IN 118405. An anonymous referee is thanked for interesting comments that have improved this manuscript.

## REFERENCES

- de Blok, W.J.G. & Walter, F. 2000, ApJ, 537, 95
- Brocklehurst, M. 1971, MNRAS, 153, 471
- Castellanos, M., Valls-Gabaud, D., Diaz, A.I., & Tenorio-Tagle, G. 2004, “How does the Galaxy work?” eds: E.J. Alfaro, E. Perez & J. Franco, Kluwer Academic Publishers, p.101
- Domgörgen, H. & Mathis. J.S. 1994, ApJ, 428, 647
- Dopita, M.A. 1993. PASAu, 10, 359
- Dopita, M. A. & Sutherland, R. 1995, ApJ, 455, 468
- Elwert, T. & Dettmar, R.-J. 2005, ApJ, 632, 277
- Galarza, V.C., Walterbos, R.A.M., & Braun, R. 1999, AJ, 118, 2775
- Greenawalt, B., Walterbos, R.A.M., Thilker, D. & Hoopes, C.G. 1998, ApJ, 506, 135
- Hidalgo-Gómez, A.M. 2004, “How does the Galaxy work?” eds: E.J. Alfaro, E. Perez & J. Franco, Kluwer Academic Publishers, p.71
- Hidalgo-Gómez, A.M. 2005 A&A, 442, 443
- Hidalgo-Gómez, A.M. 2006, AJ, 131, 2078
- Hidalgo-Gómez, A.M., & Olofsson, K. 1998, A&A, 334, 45
- Hidalgo-Gómez, A.M., Olofsson, K. & Masegosa, J., 2001, A&A, 367, 388 (HGMO)
- Hidalgo-Gómez, A.M. & Olofsson, K. 2002, A&A, 389, 836
- Hidalgo-Gómez, A.M. & Ramírez-Fuentes, D., A&A submitted
- Hidalgo-Gómez, A.M. & Flores-Fajardo, N. 2007, AJ submitted
- Hodge, P., Lee, M.G., & Kennicutt, R.C.Jr. 1989, PASP, 101, 32
- Hoppes, C. G. & Walterbos, R.A.M. 2003, ApJ, 586, 902
- Hunter, D.A. & Gallagher, J.S. 1990, ApJ, 362, 480
- Hunter, D. A., & Elmegreen, B.G. 2004, AJ, 128, 2170

- Karachentsev, I.D. 2005, *AJ*, 129, 178
- Martin, C.L. 1997, *ApJ*, 491, 561
- Mathis, J.S. 1986, *ApJ*, 301, 423
- McCall, M.L., Rybski, P.M., & Shields, G.A. 1985, *ApJS*, 57, 1
- Miller, S.T. & Veilleux, S. 2003, *ApJ*, 592, 79
- O’Dell, C.R. 2001, *ARA&A*, 39, 99
- Osterbrock, D.E. 1989, *Astrophysics of Gaseous Nebulae and Active Galactic Nuclei*, (University Science Books, Mill Valley, CA)
- Otte, B. & Dettmar, R.-J. 1999, *A&A*, 343, 705
- Otte, B., Reynolds, R.J., Gallagher, J.S. III, & Ferguson, A.M.N. 2001, *ApJ*, 560, 207
- Otte, B., Gallagher, J.S.III, & Reynolds, R.J. 2002, *ApJ*, 572, 823
- Peimbert, A., Peimbert, M. & Ruiz, M.T. 2005, *ApJ*, 634,1056
- Petuchowski, S.J. & Bennett, C.L. 1993, *ApJ*, 405, 591
- Petuchowski, S.J. & Bennett, C.L. 1995, *ApJ*, 438, 735
- Polcaro, V.F., Rossi, C., Norci, L., & Viotti, R. 1995, *A&A*, 303, 211
- Rand, R.J. 1998, *ApJ*, 501, 137
- Relaño, M., Peimbert, M., & Beckman, J. 2002, *ApJ*, 564, 704
- Reynolds, R.J. 1984, *ApJ*, 282, 191
- Reynolds, R.J., Haffner, L.M.,& Tufte, S.L. 1999, *ApJL*, 525, 21
- Rola, C. & Pelat, D. 1994, *A&A*, 287, 676
- Savage, B.D. & Mathis, J.S. 1979, *ARA&A*, 17, 73
- Slavin, J.D, Shull, J.M. & Begelman, M.C. 1993, *ApJ*, 407, 83
- Strömgren, B. 1939, *ApJ*, 89, 526
- Tüllman, R., & Dettmar, R.-J. 2000, *A&A*, 362, 119



de Vaucouleurs, G., de Vaucouleurs, A., Corwin, H.G., et al. 1991, Third Reference Catalogue of Bright Galaxies (Springer-Verlag)

Veilleux, S. & Osterbrock, D.E. 1987, ApJS, 63, 295

Wyder, T.K. 2001, AJ, 122, 2490

Wood, K., & Mathis, J.S. 2004, MNRAS, 353, 1126

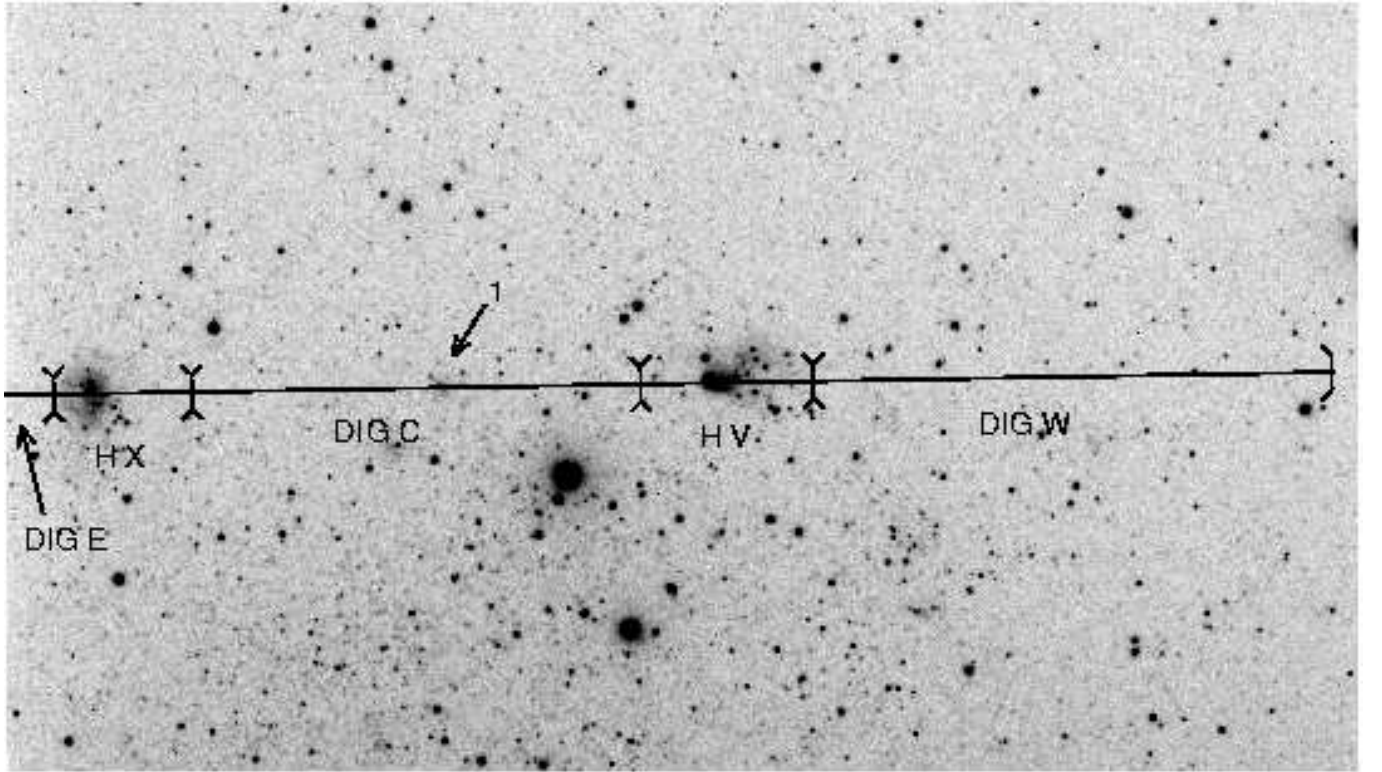


Fig. 1.— VLT image of the northern part of NGC 6822. The image of  $392'' \times 224''$  is centered at  $\alpha=19^h 44^m 53.4^s$ ,  $\delta=-14^\circ 43' 15''$ . The total area of the five regions adds up to  $400'' \times 0.51''$  (see text). Most of the extraction aperture is shown in the figure; however  $16''$  of the DIG E region are not in the figure. Point “1” indicates a region of low hydrogen emission (see text).

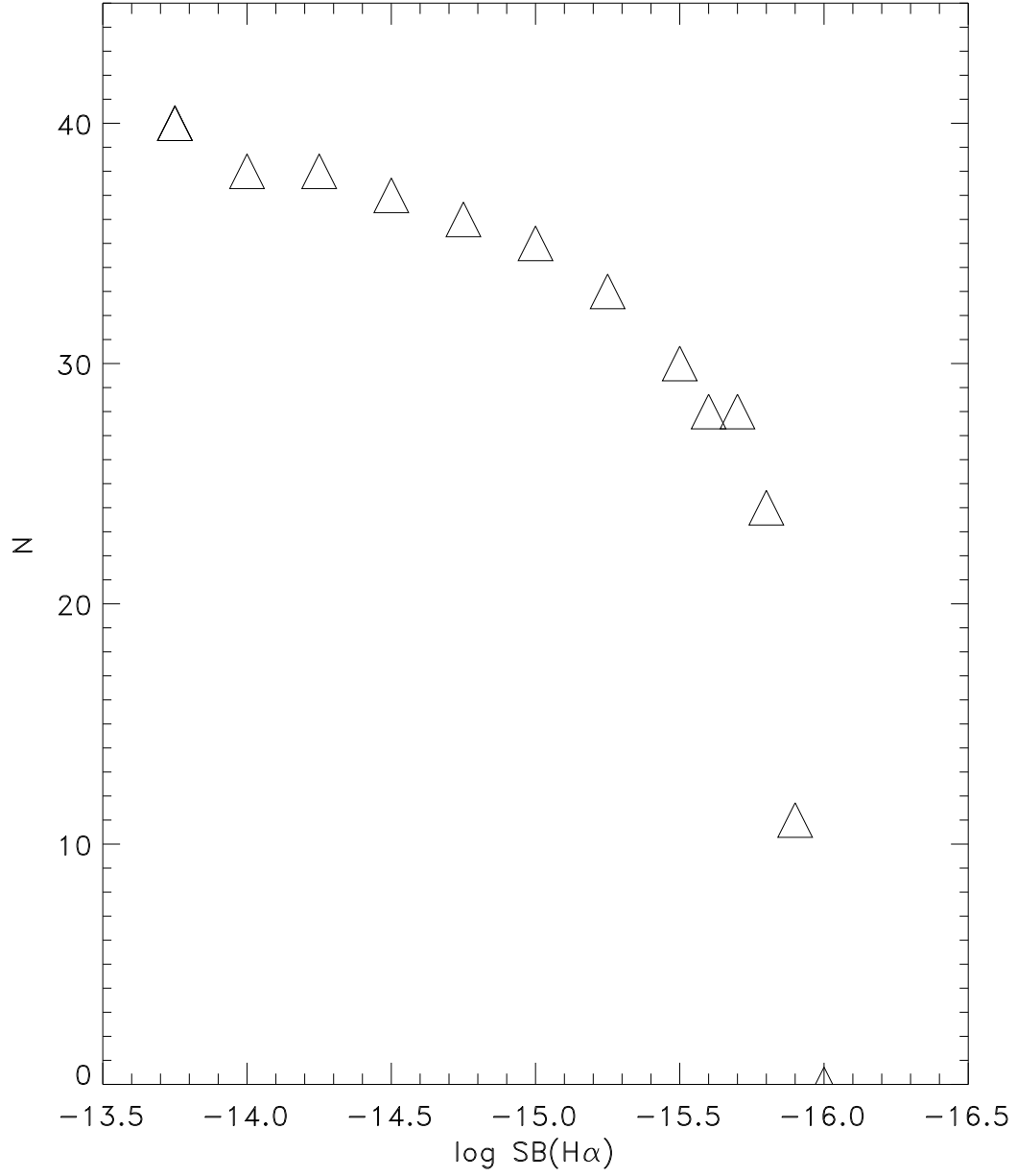


Fig. 2.— Cumulative function of the surface brightness in  $H\alpha$  for all the data along the slit in NGC 6822. The turnoff point represents the limiting surface brightness value between DIG and H II regions. For this galaxy, it is -15.3.

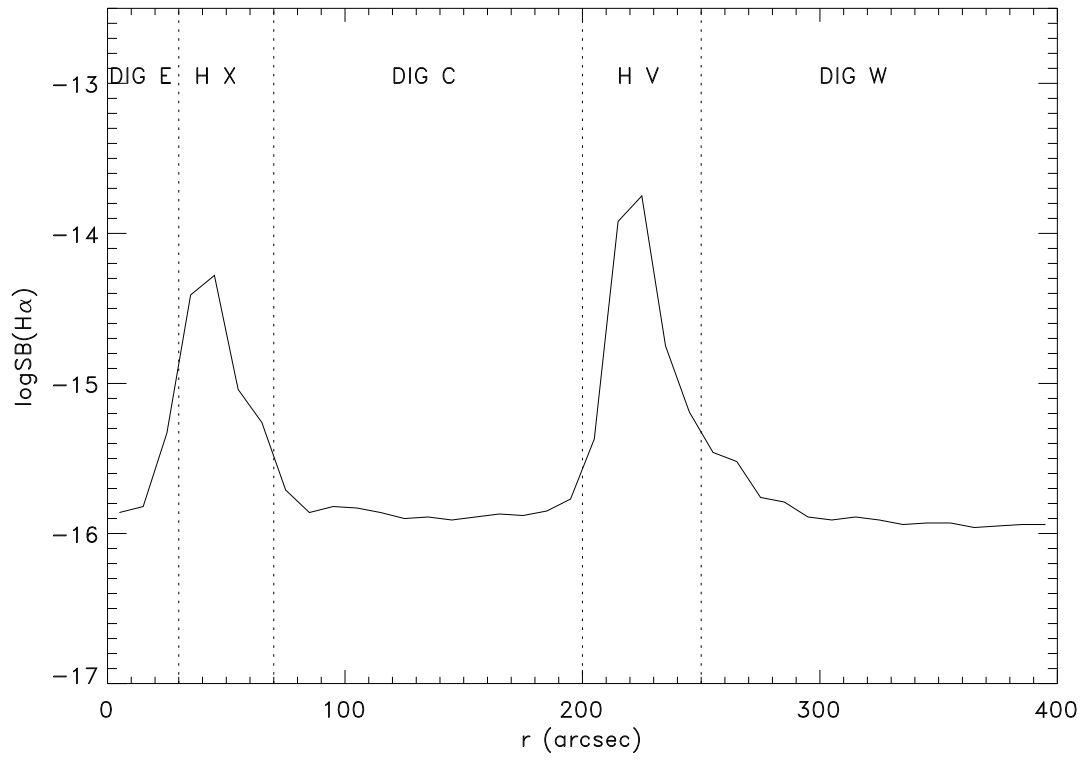


Fig. 3.— SB( $H\alpha$ ) along the slit position in NGC 6822. The dotted lines include the H II regions. East is to the left.

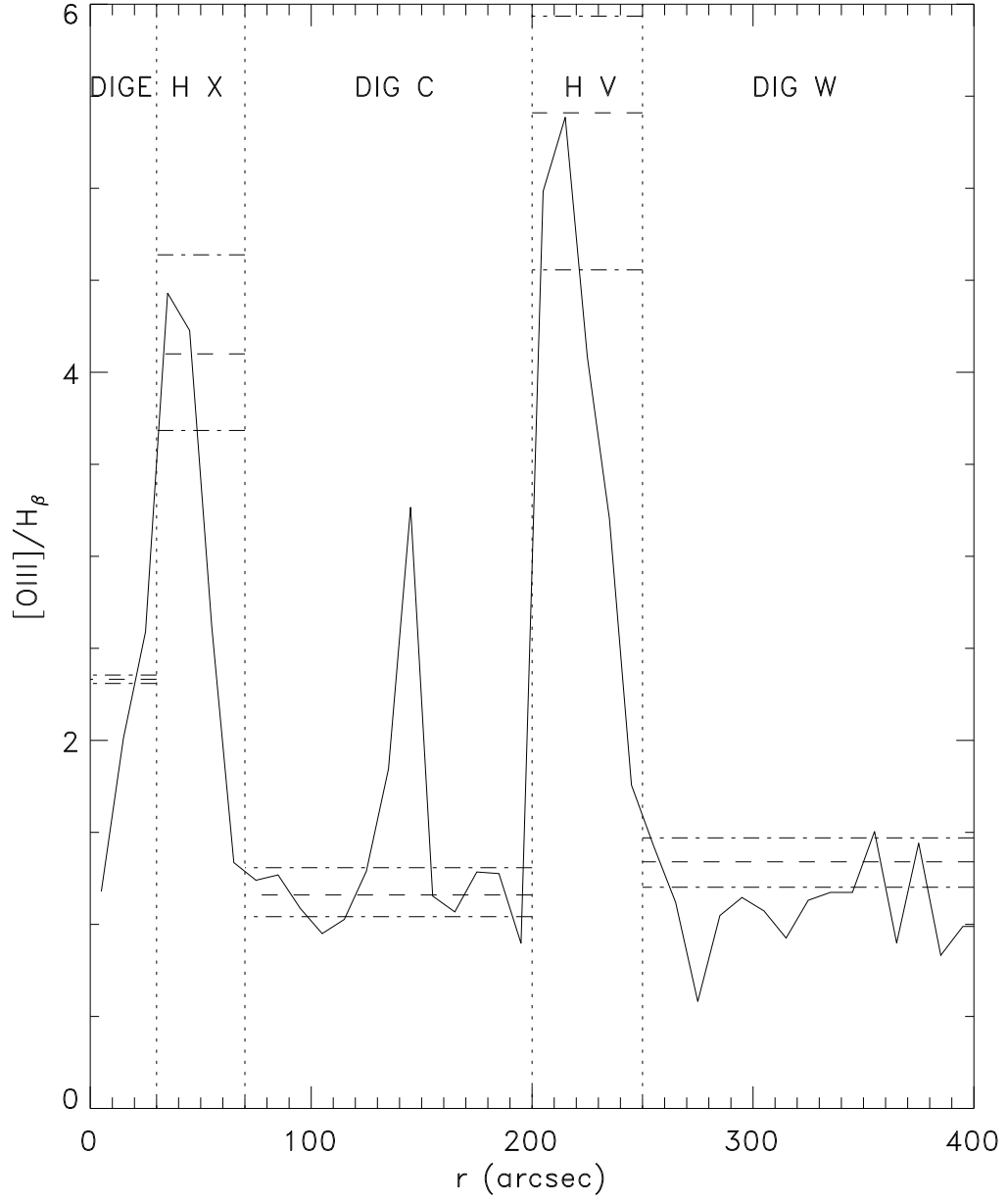


Fig. 4.— Excitation, defined as  $[O III]/H\beta$ , along the slit. The dotted lines include the H II regions, while the dashed lines correspond to the integrated spectra values with error bars (*dot – dashed* lines). Orientation is as in Fig. 3.

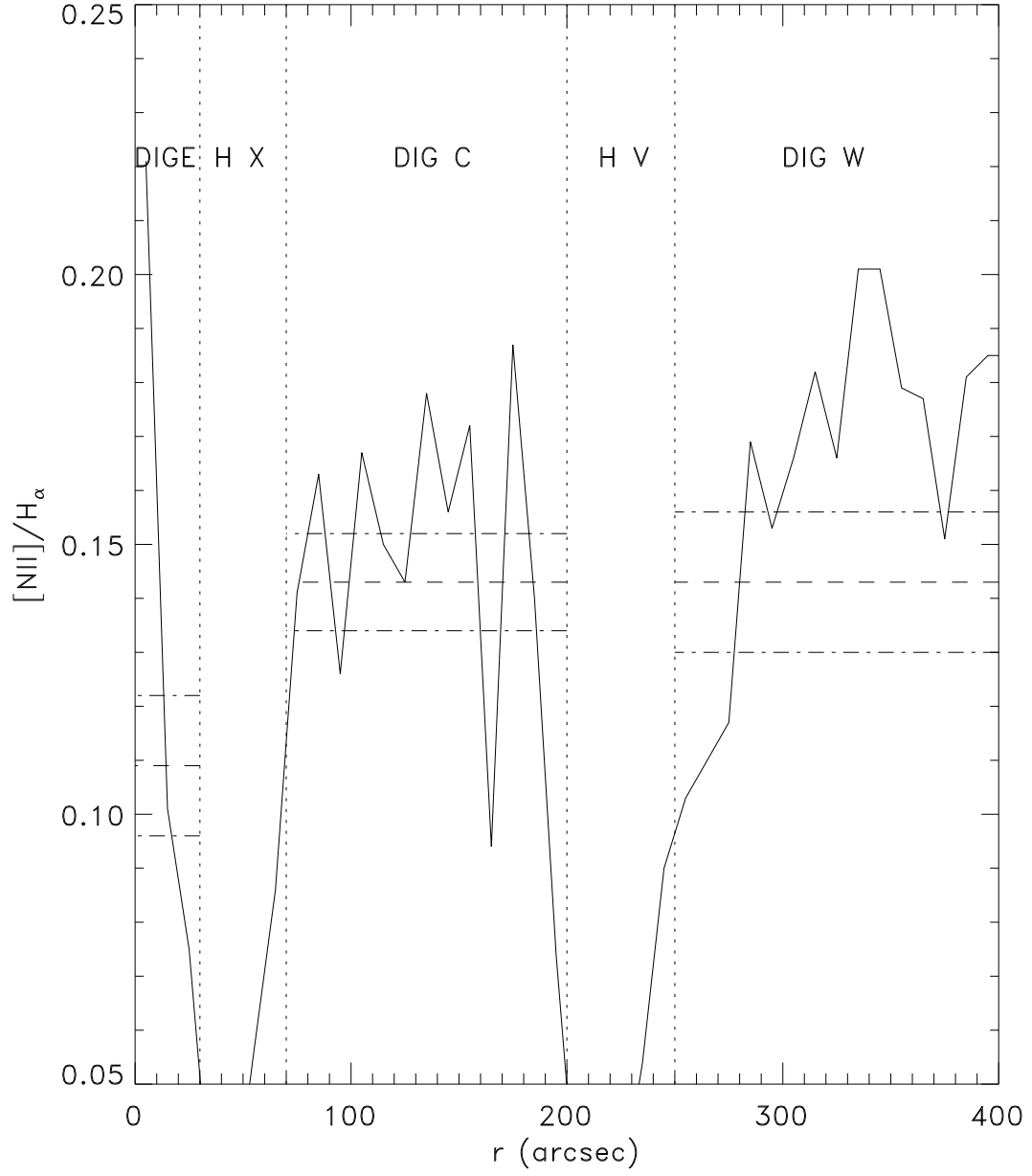


Fig. 5.— [N II]  $\lambda 6584$ /H $\alpha$  ratio along the slit. Symbols and orientation are as in Fig. 4.

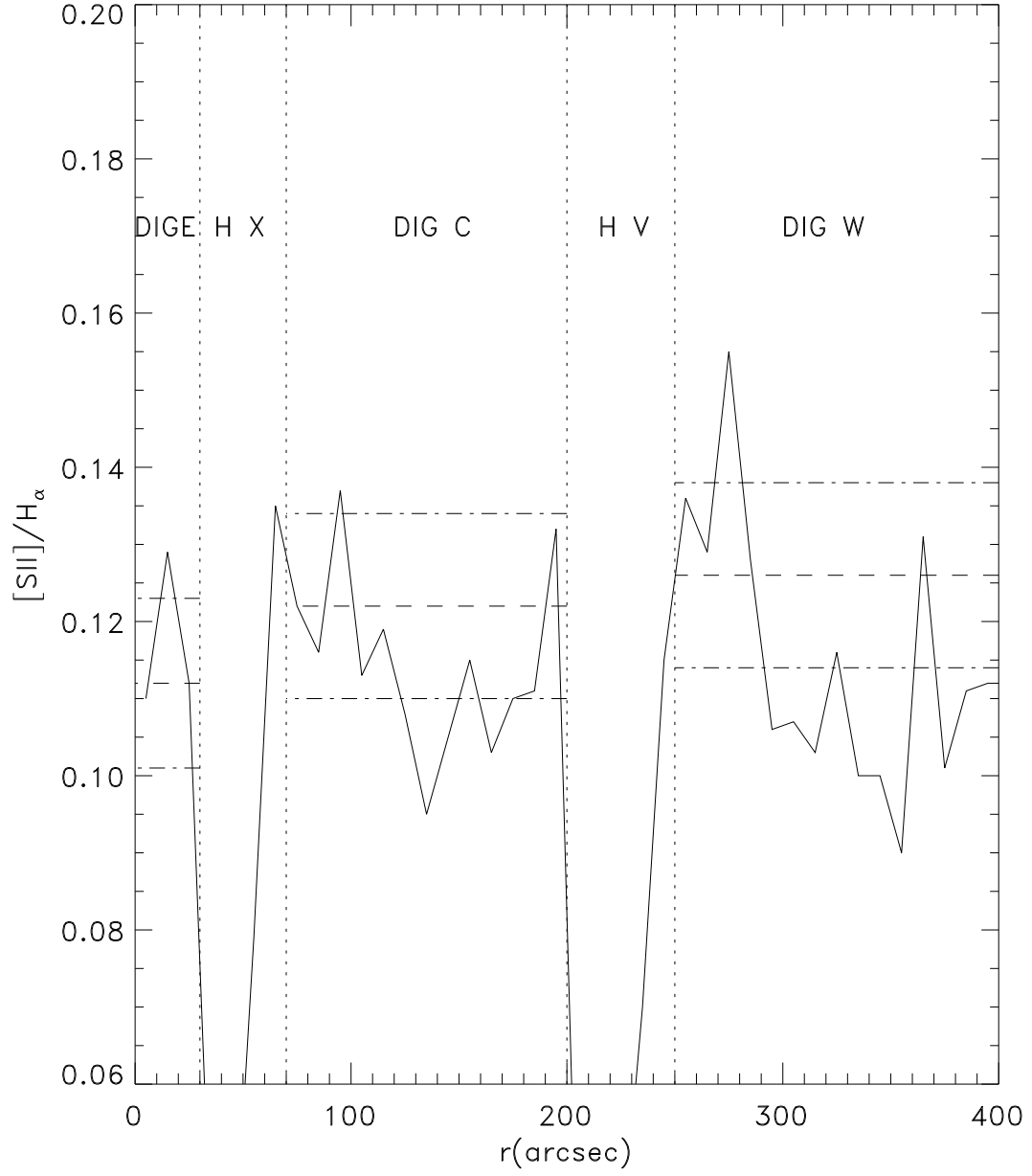


Fig. 6.— [SII]  $\lambda 6717$ /H $\alpha$  ratio along the slit. Symbols and orientation are as in Fig. 4.

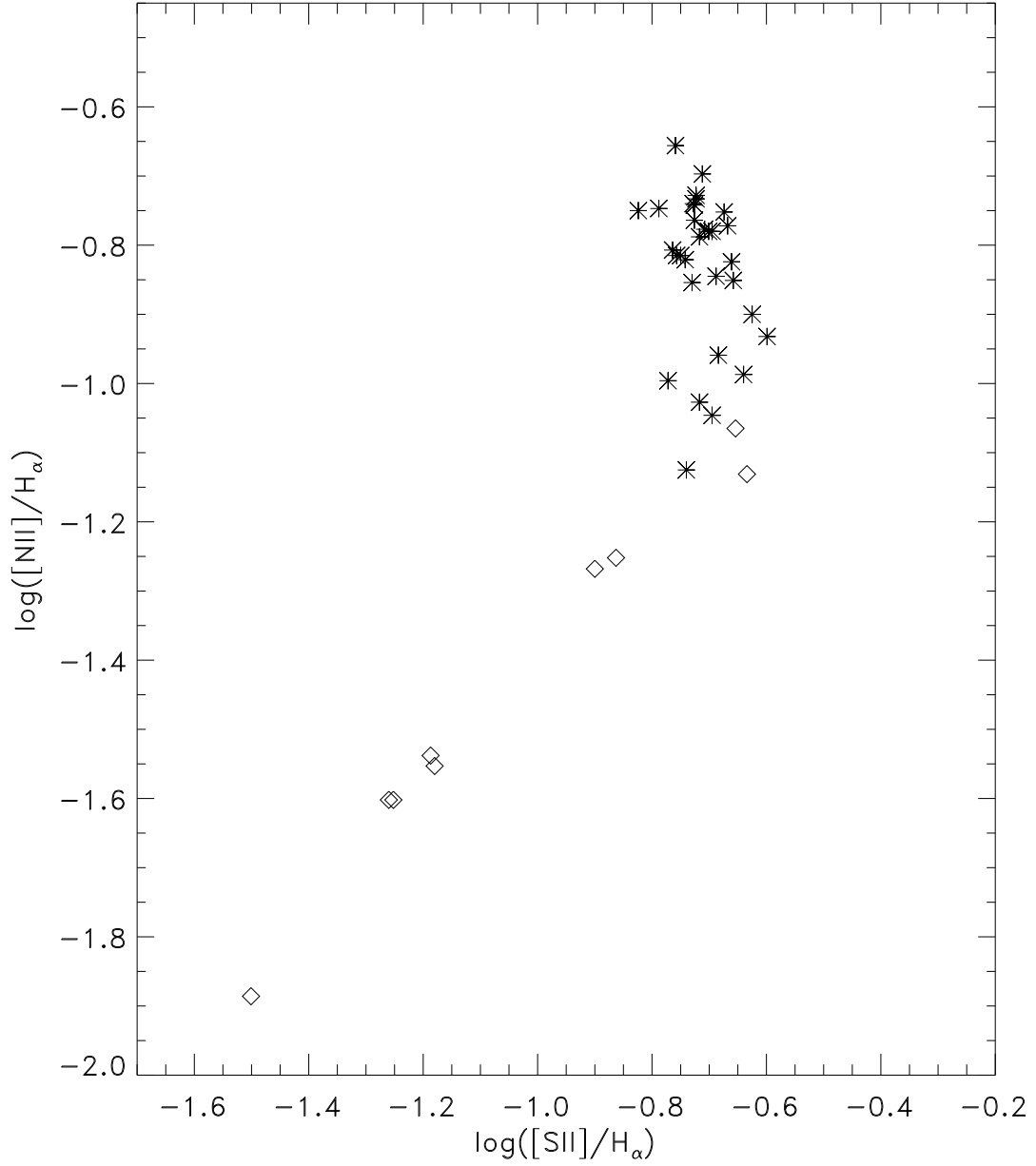


Fig. 7.—  $\log([\text{N II}]\lambda 6584/\text{H}\alpha)$  vs.  $\log([\text{S II}]\lambda 6717/\text{H}\alpha)$ . H II regions (*diamonds*) show a perfect correlation, but the DIG locations (*asterisk*), are scattered; the opposite is observed in spiral galaxies.



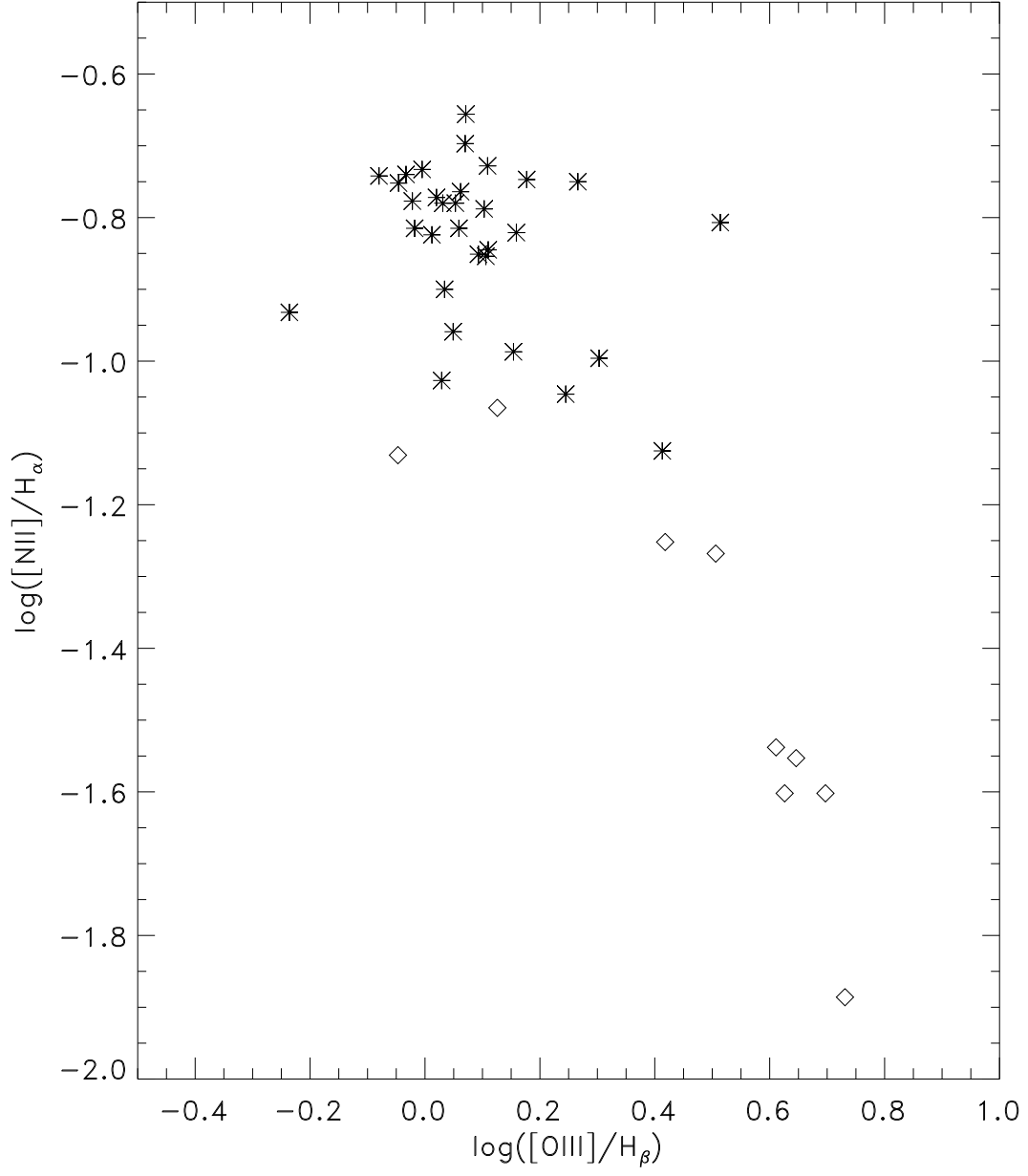


Fig. 8.—  $\log([\text{O III}]/\text{H}\beta)$  vs.  $\log([\text{N II}]\lambda 6584\text{\AA}/\text{H}\alpha)$  for all the data points. Symbols are as in Fig. 7. The H II regions follow a correlation, but the DIG locations are scattered, with the majority of them between  $-0.1$  and  $0.3$  in  $\log[\text{O III}]/\text{H}\beta$ .

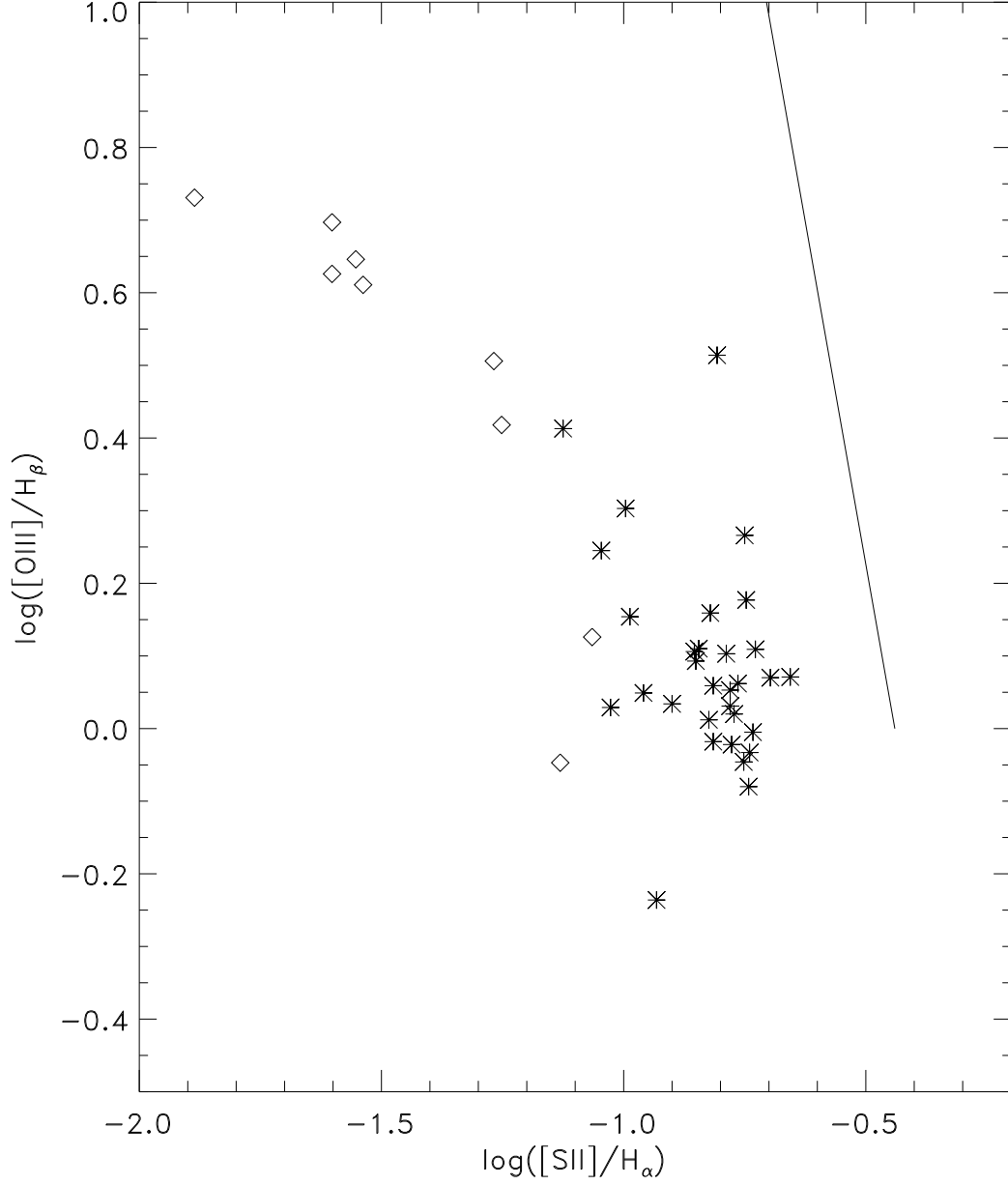


Fig. 9.—  $\log([\text{S II}]\lambda\lambda(6717+6731)/\text{H}\alpha)$  vs.  $\log([\text{O III}]/\text{H}\beta)$ . The line corresponds to the shock model, without precursors, of Dopita & Sutherland (1995). Symbols are as in Fig. 7. None of the DIG or the H II locations is situated in the shocked region (*to the right of the line*).

Table 1: Total values of the line ratios (extinction corrected) from the integrated spectra.

Parameter	DIG W	Hubble V	DIG C	Hubble X	DIG E
[OIII] $\lambda$ 5007/H $\beta$	1.34 $\pm$ 0.07	5.41 $\pm$ 0.3	1.16 $\pm$ 0.06	4.10 $\pm$ 0.2	2.332 $\pm$ 0.1
He I $\lambda$ 5875/H $\alpha$	0.07 $\pm$ 0.03	0.036 $\pm$ 0.003	0.06 $\pm$ 0.03	0.040 $\pm$ 0.003	0.06 $\pm$ 0.03
[NII] $\lambda$ 6583/H $\alpha$	0.14 $\pm$ 0.01	0.017 $\pm$ 0.001	0.14 $\pm$ 0.005	0.031 $\pm$ 0.001	0.109 $\pm$ 0.009
[SII] $\lambda$ 6717/H $\alpha$	0.123 $\pm$ 0.006	0.028 $\pm$ 0.001	0.120 $\pm$ 0.006	0.045 $\pm$ 0.002	0.112 $\pm$ 0.006
[SII] $\lambda$ 6717/[SII] $\lambda$ 6731 $\text{\AA}$	1.44 $\pm$ 0.09	1.6 $\pm$ 0.07	1.4 $\pm$ 0.07	1.41 $\pm$ 0.07	1.829 $\pm$ 0.09
[NII] $\lambda$ 6584/[SII] $\lambda$ 6717 $\text{\AA}$	1.14 $\pm$ 0.1	0.62 $\pm$ 0.05	1.17 $\pm$ 0.06	0.69 $\pm$ 0.05	0.97 $\pm$ 0.09
$C_\beta$	2.75 $\pm$ 0.01	0.44 $\pm$ 0.005	2.71 $\pm$ 0.01	0.08 $\pm$ 0.005	0.708 $\pm$ 0.001
$T_e$ DIG (N)	9228	-	8578	-	9936
$T_e$ DIG (O)	10202	-	9261	-	9698
S/N (H $\alpha$ )	8	23	9	21	6